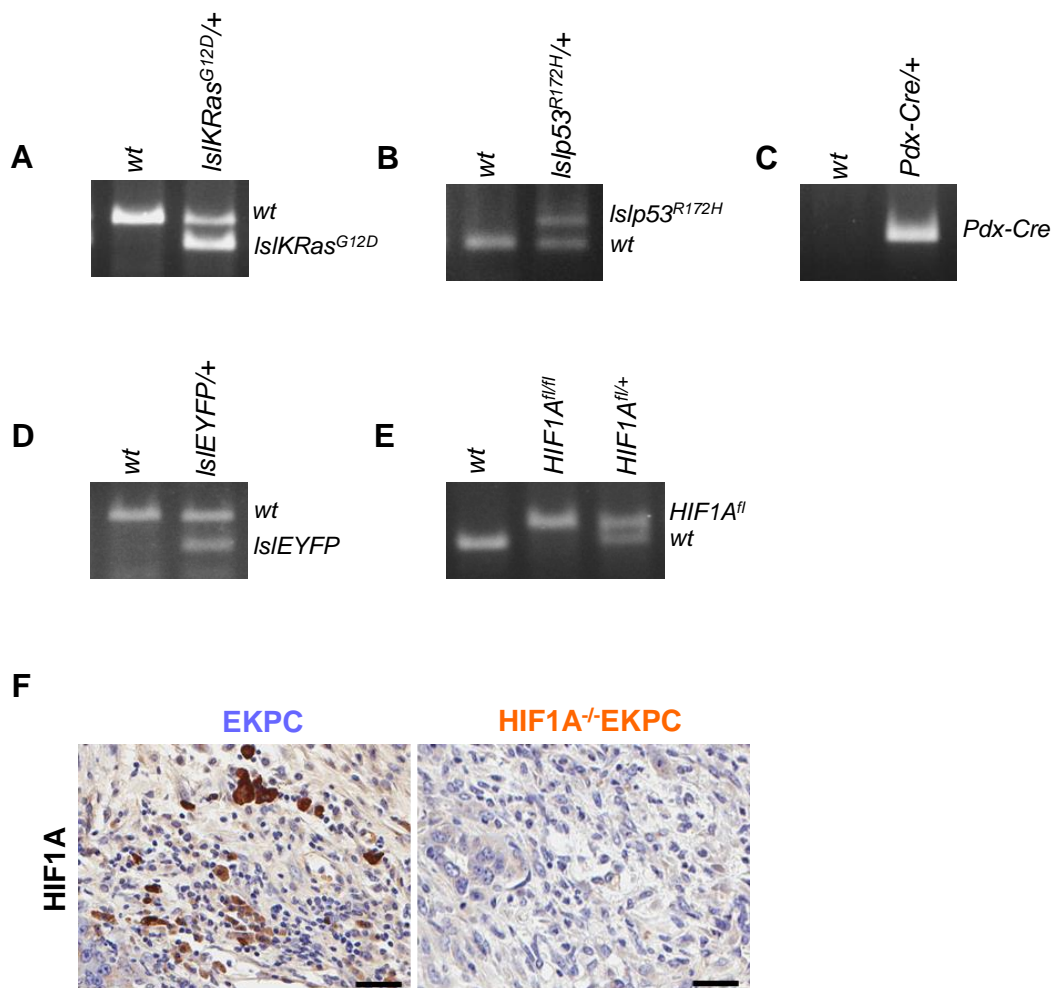
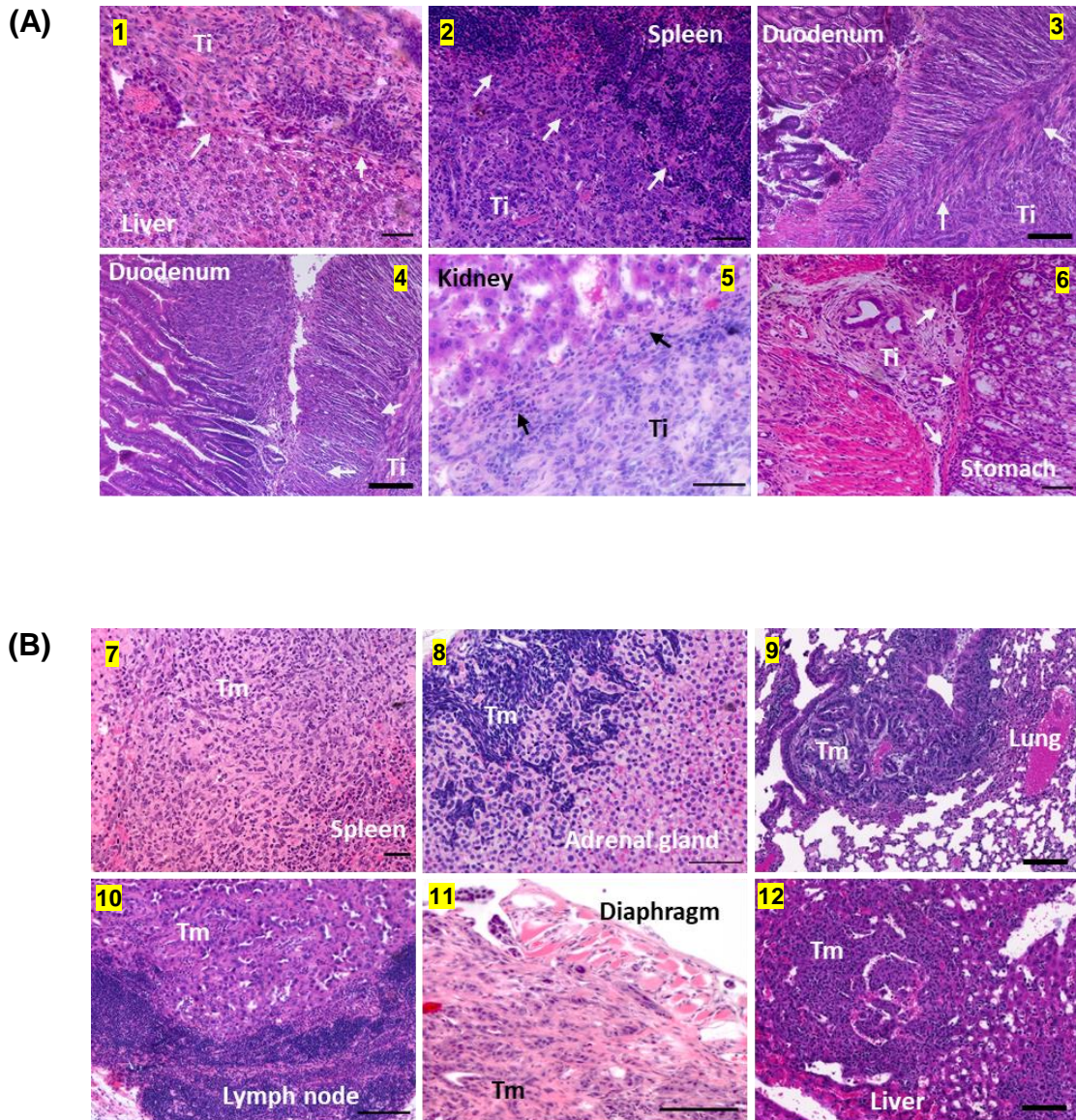


Supplementary Figure 1 :



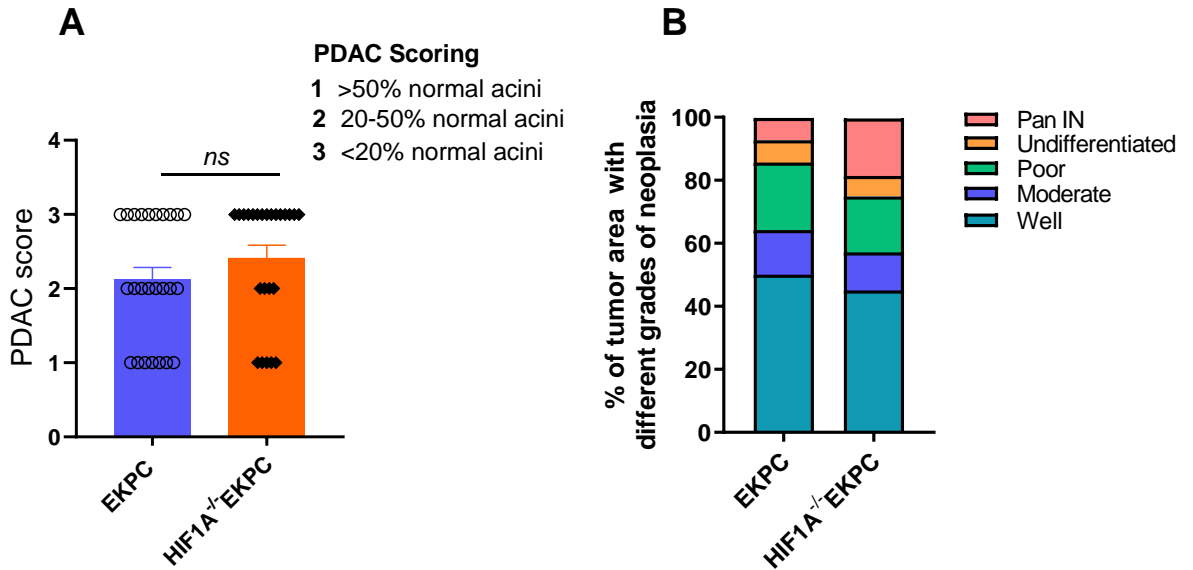
Supplementary Figure 1: Genotyping of EKPC and HIF1A^{-/-}EKPC mice by PCR analysis of genomic DNA extracted from tail tips. **(A)** *LSL-Kras^{G12D}/+* **(B)** *LSL-p53^{R172H}/+* **(C)** *Pdx-Cre/+* **(D)** *LSL-EYFP/+* **(E)** HIF1A^{wt}, HIF1A^{fl/fl} and HIF1A^{fl/+} mice. **(F)** Representative images of immunohistochemistry staining for HIF1A in EKPC and HIF1A^{-/-} EKPC tumor sections. Scale bar, 50 μ m.

Supplementary Figure 2 :



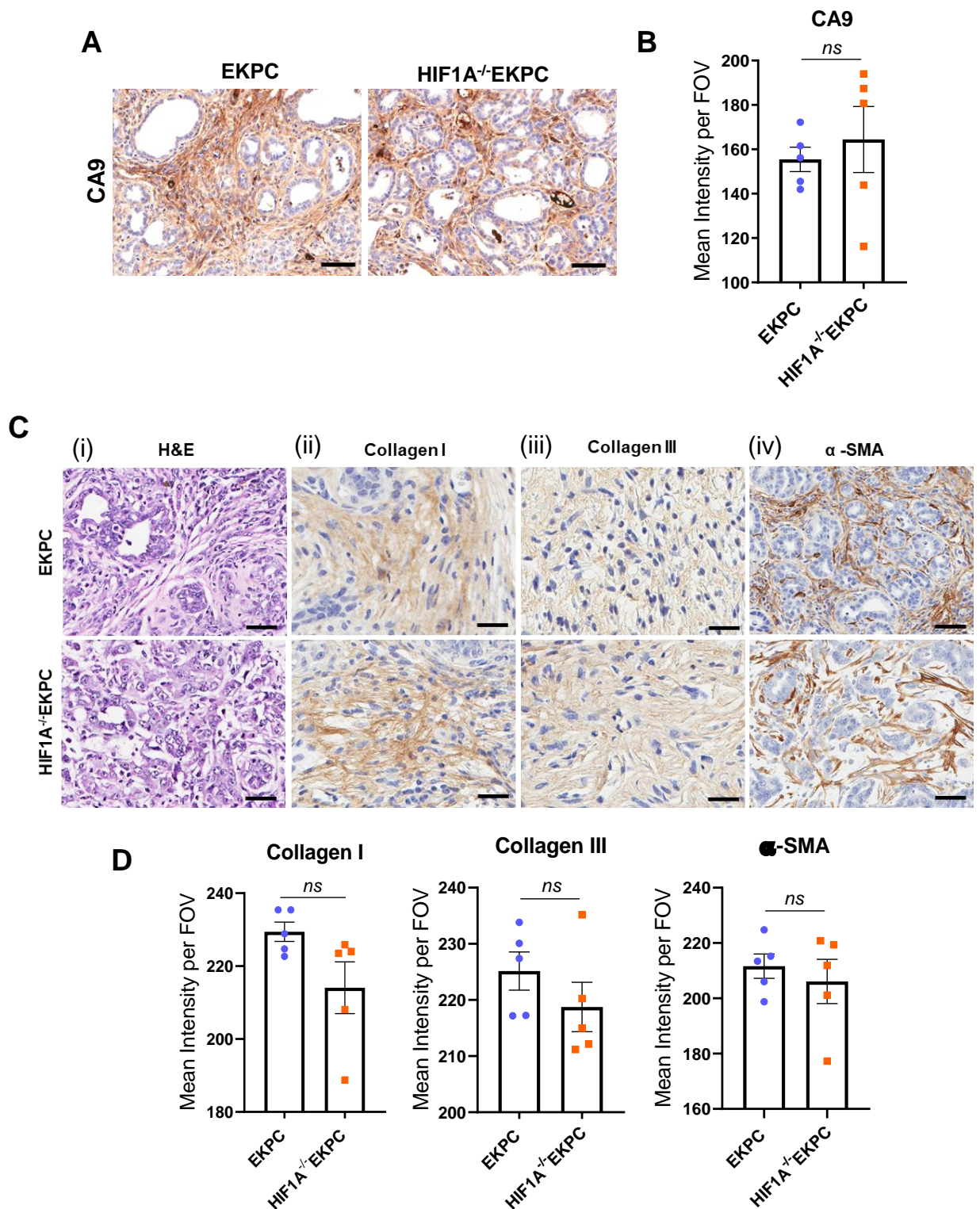
Supplementary Figure 2: (A) Hematoxylin and eosin (H&E) staining of different organs of HIF1A^{-/-}EKPC mice showing tumor invasion (Ti) (1-6); (1) Liver (2) Spleen (3,4) Duodenum (5) Kidney (6) Stomach **(B)** Tumor metastatic lesion (Tm) (7-12) ; (7) Spleen (8) Adrenal gland (9) Lung (10) Lymph node (11) Diaphragm (12) Liver. The boundaries of invasion is shown by arrows. Scale bar = 50 μM.

Supplementary Figure 3 :



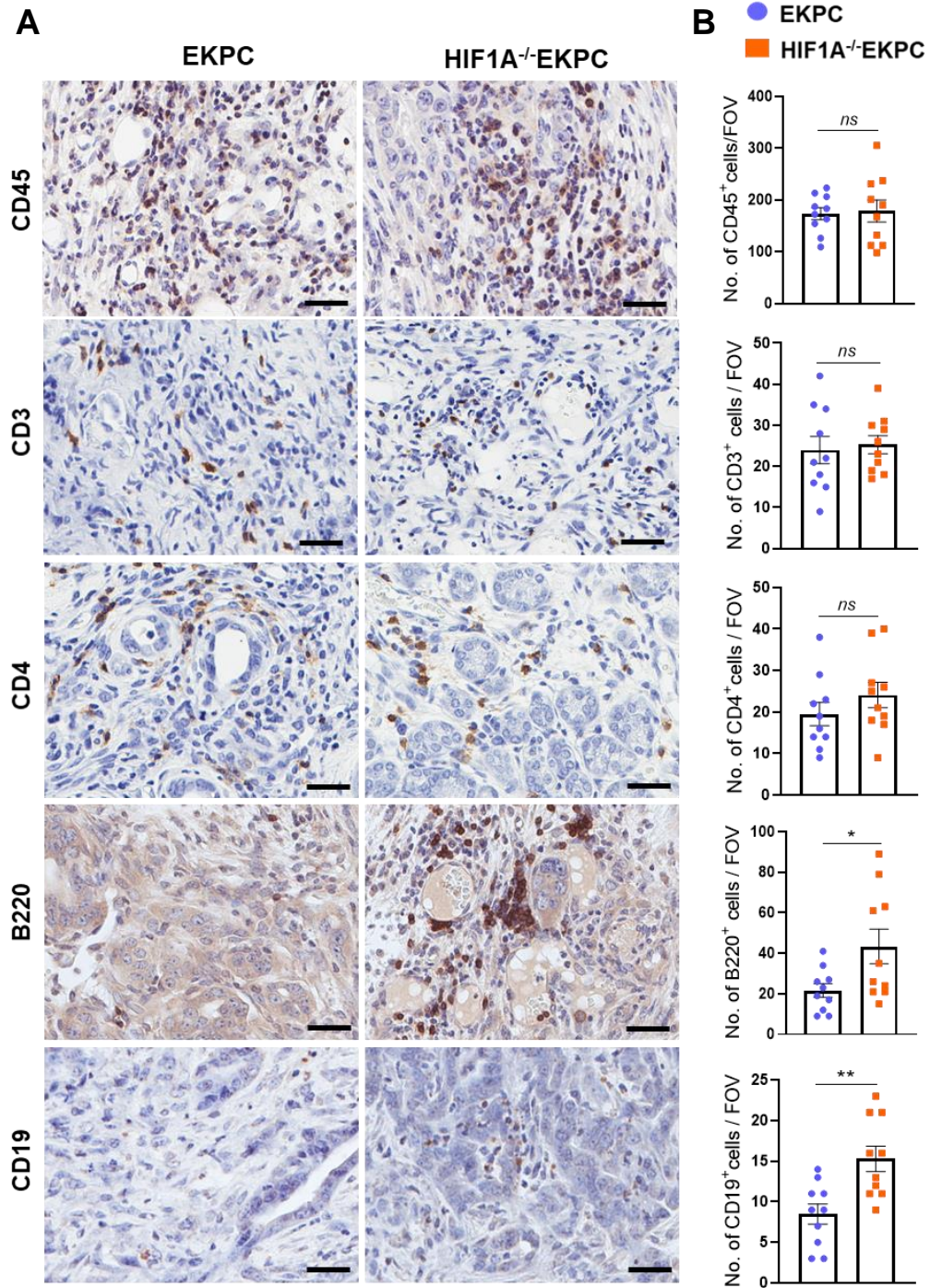
Supplementary Figure 3: (A) Scoring of PDACs derived from EKPC (n=25) and HIF1A^{-/-}EKPC (n=24) mice. PDAC scoring was determined on basis of disease severity (1 for >50% normal acini, 2: 20-50% normal acini and 3: <20% normal acini) **(B)** Comparative profile of histological grading of EKPC and HIF1A^{-/-}EKPC tumor samples at the endpoint. The area within tumors were classified using the standard pathological grading scheme into either PanINs and well differentiated, moderately differentiated, poorly differentiated and anaplastic or undifferentiated.

Supplementary Figure 4 :



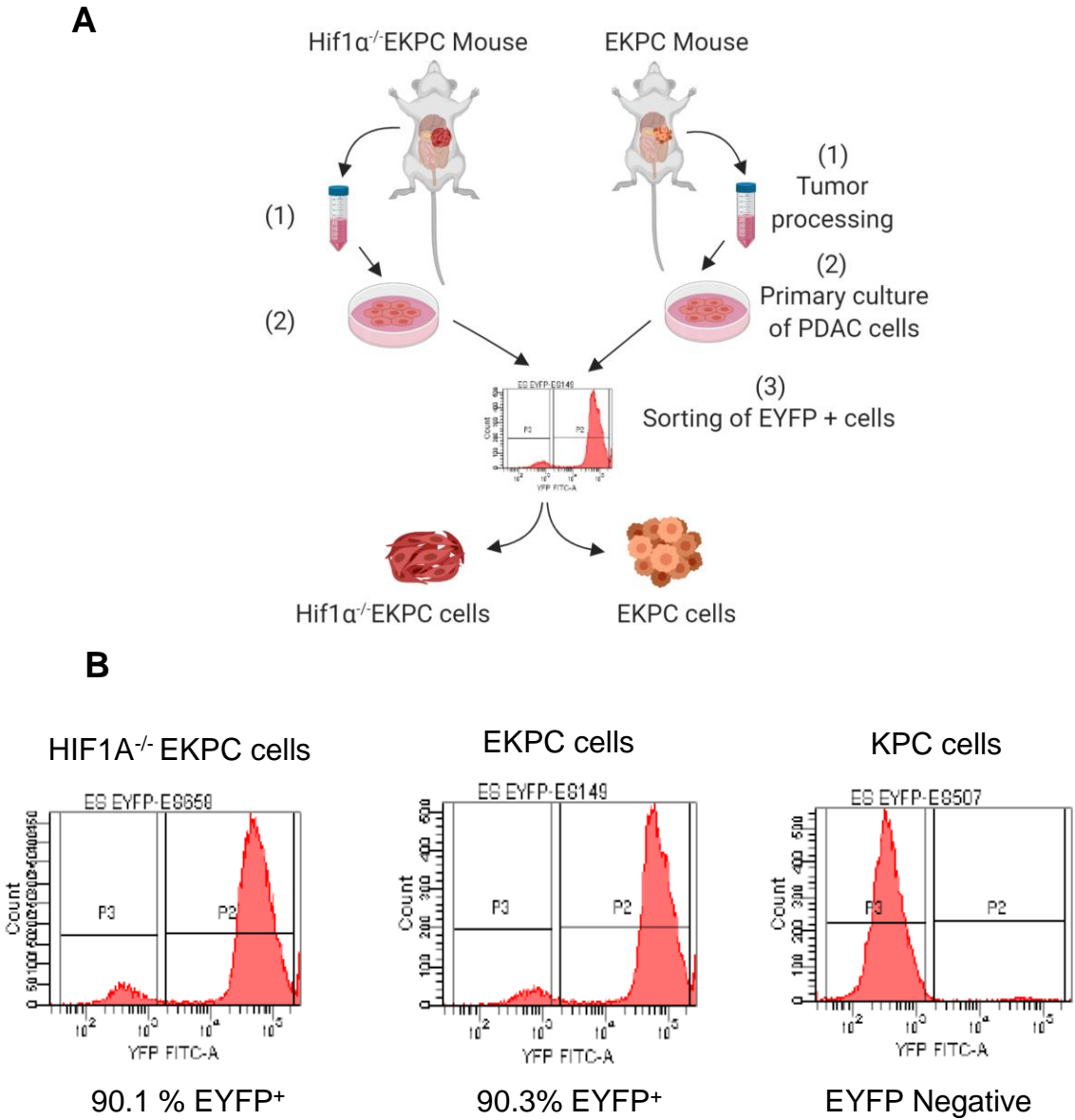
Supplementary Figure 4: (A) Representative images of immunohistochemistry for Carbonic Anhydrases 9 (CA9) expression in EKPC and HIF1A^{-/-}EKPC tumors. Scale bar, 50 μm (B) Quantification of CA9 staining as mean intensity per field of vision in EKPC and HIF1A^{-/-}EKPC tumor sections (n = 5 field of vision for each section). (C) (i) Representative images of hematoxylin and eosin (H&E) stained slides of EKPC and Hif1α^{-/-}EKPC PDACs with stroma content. (ii-iv) Immunohistochemistry for Collagen type I, Collagen type III and α-SMA expression in PDAC tumors. Scale bar = 50. (D) Quantification of Collagen type I, Collagen Type III and α-SMA staining as mean intensity per field of vision in EKPC and HIF1A^{-/-}EKPC tumor sections (n = 5 field of vision for each section). The data are shown as the mean ± s.e.m. P values were determined by unpaired t test. ns, not significant.

Supplementary Figure 5 :



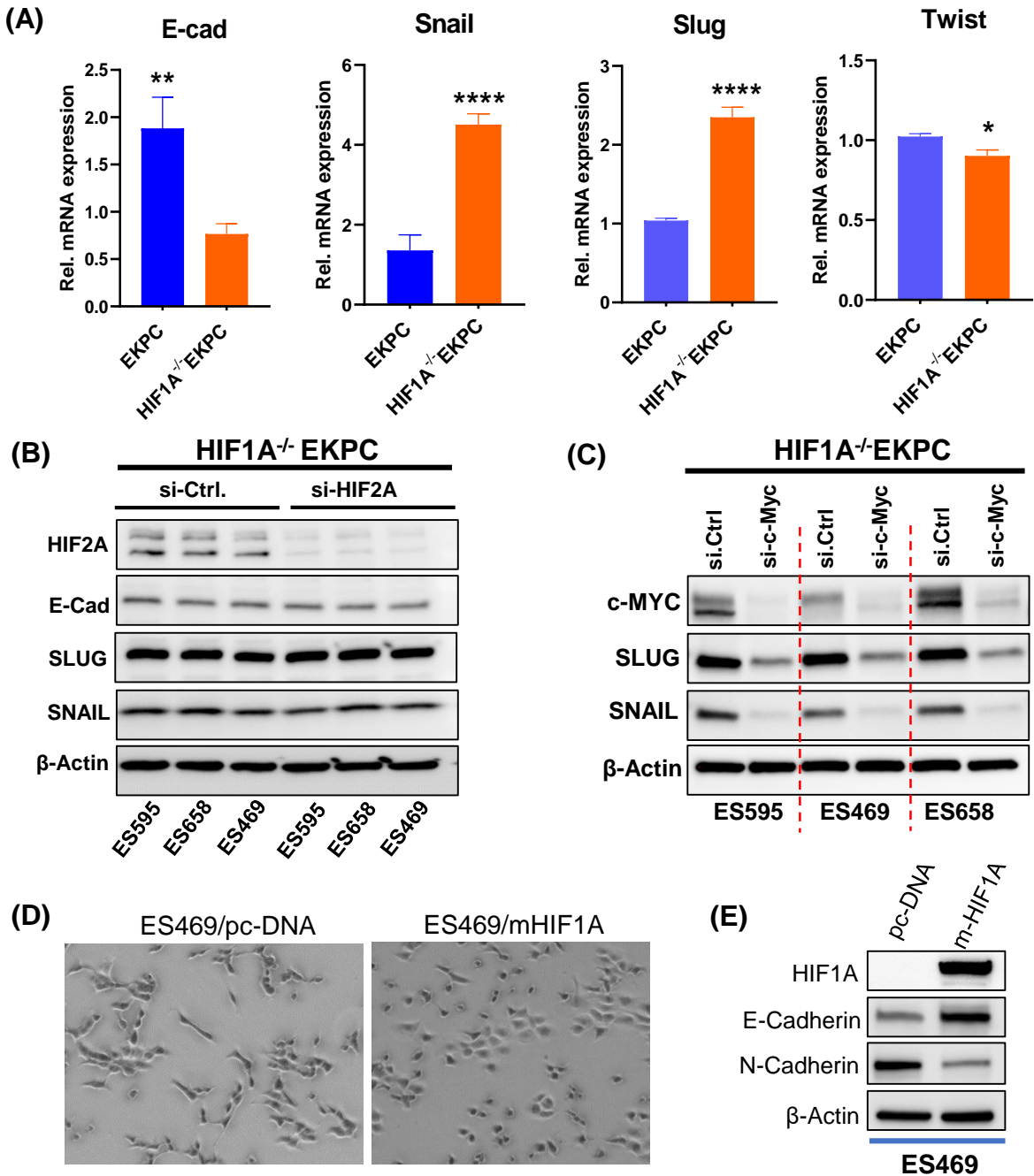
Supplementary Figure 5: (A) Immunohistochemical staining for CD45, CD3, CD4, B220 and CD19 positive cells in PDAC sections from EKPC and HIF1A^{-/-} EKPC mice. Scale bar, 50 μ m **(B)** Quantification of CD45+, CD3+, CD4+, B220+ and CD19+ cells in EKPC and HIF1A^{-/-} EKPC tumor sections (n = 10 field of vision). The data are shown as the mean \pm s.e.m. P values were determined by unpaired t test. ns, not significant, *P<0.05, **P < 0.01.

Supplementary Figure 6 :



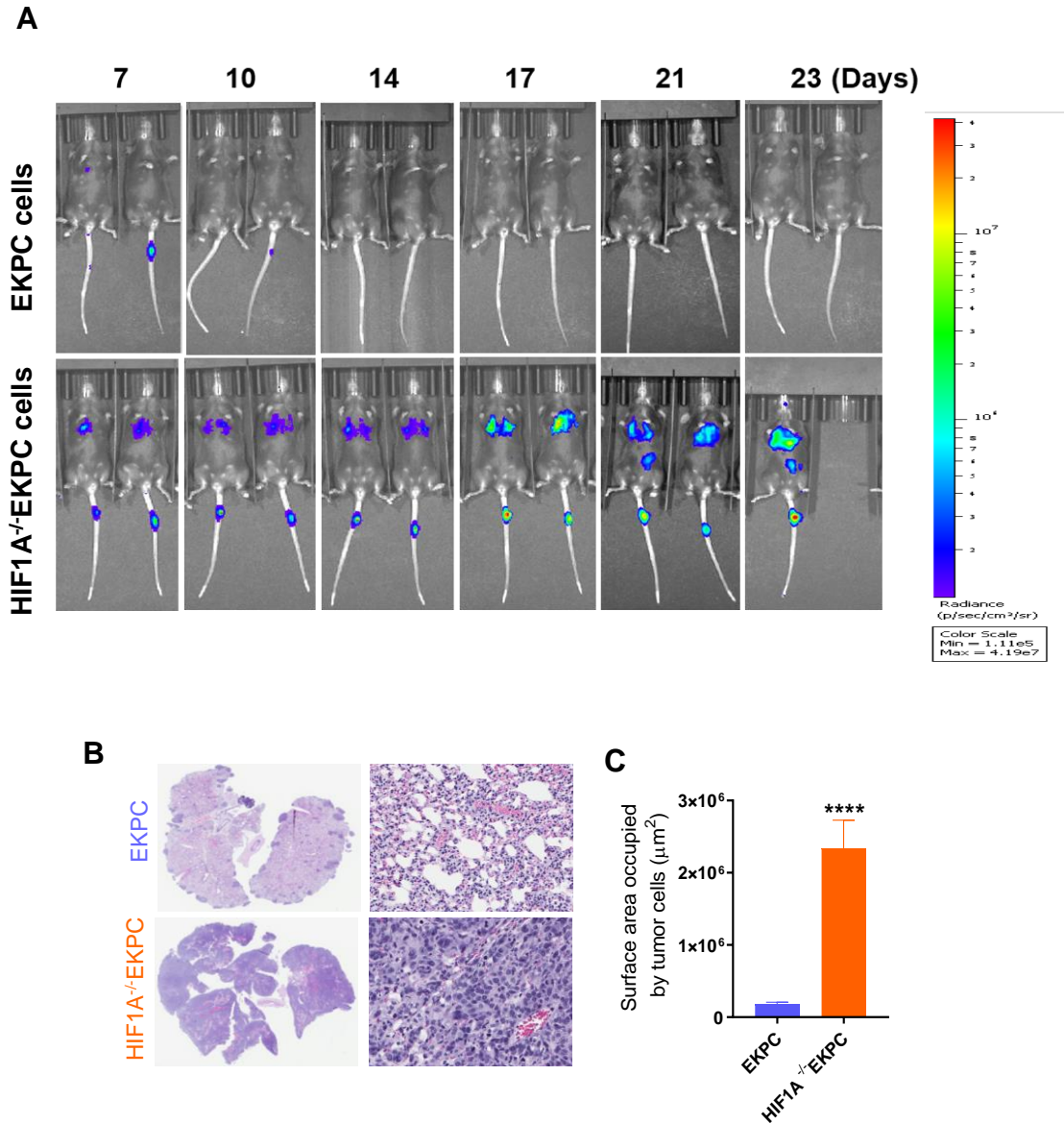
Supplementary Figure 6: Generation of PDAC derived EKPC and HIF1A $^{-/-}$ EKPC cells **(A)** Schematics of generating HIF1A $^{-/-}$ EKPC and EKPC cells derived from murine PDACs. **(B)** Purification and isolation of EYFP $^{+}$ cells from murine PDAC by flow sorting; the purity of the EYFP $^{+}$ population was confirmed by repeat FACS.

Supplementary Figure 7 :



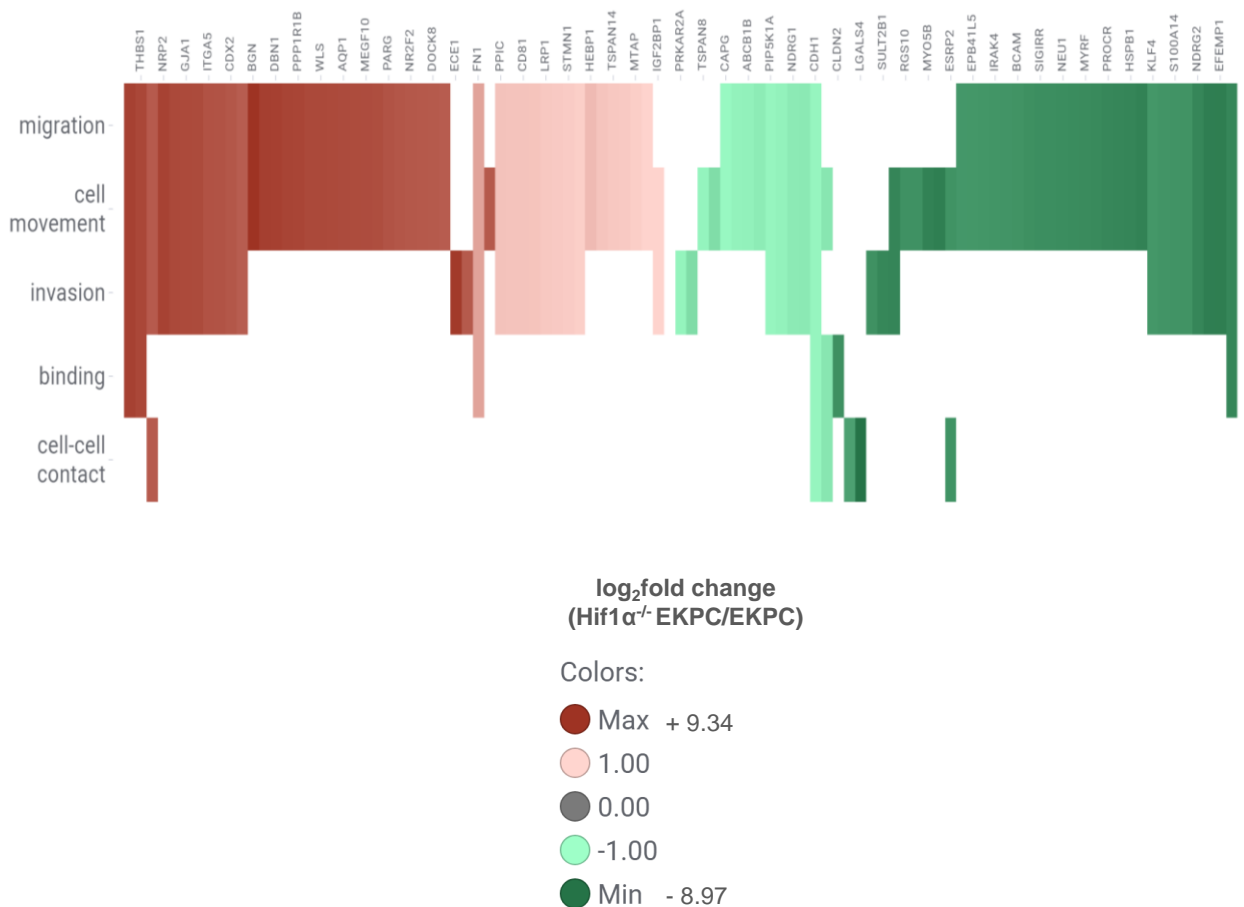
Supplementary Figure 7: (A) Relative gene expression level for EMT markers (E-cad, Snail, Slug and Twist) in EKPC (blue) and HIF1A^{-/-}EKPC (orange) cells normalized with GAPDH expression; n=3 biologically independent experiments; * $P < 0.05$, ** $P < 0.005$, **** $P < 0.0001$ by unpaired t test. **(B)** Western blot analysis of HIF2A, E-Cad, Snail and Slug in three different HIF1A^{-/-}EKPC biological replicates transfected with si-Ctrl. and si-Hif2a. **(C)** Western blot analysis of c-Myc, Snail and Slug in three different HIF1A^{-/-}EKPC biological replicates transfected with si-Ctrl and si-c-Myc. β -actin was used as loading control. **(D)** Bright field image of HIF1A^{-/-}EKPC cell line (ES469; elongated and mesenchymal morphology) and ES469 cells stably overexpressing a mutant version of Hif1 α (P402A/P577A/N813A) which is stable and active in normoxic conditions (rounded and epithelial morphology). **(E)** A comparative immunoblot analysis of HIF1A, E-Cadherin, N-Cadherin in ES469 cells with and without ectopic HIF1A expression.

Supplementary Figure 8 :



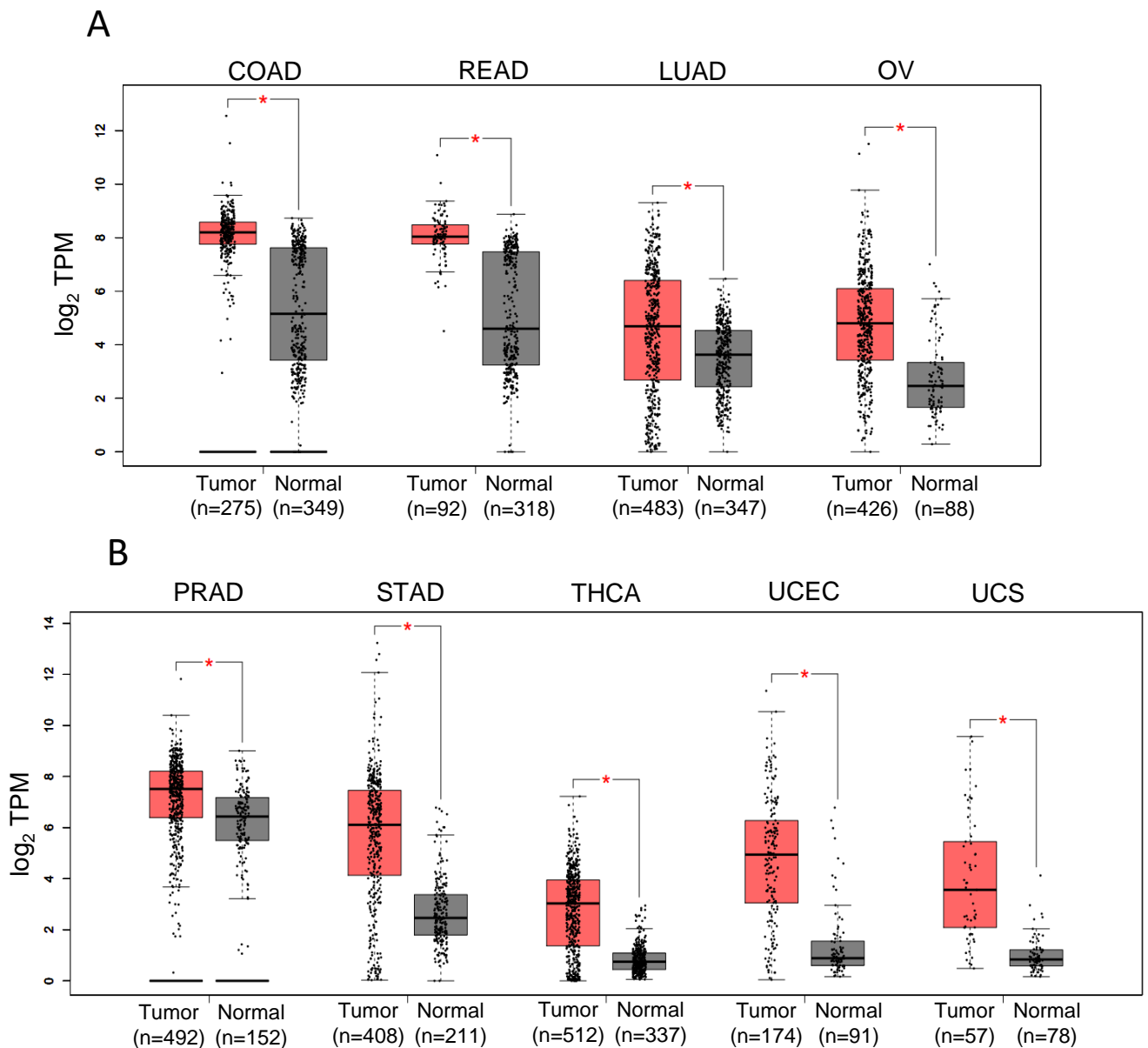
Supplementary Figure 8: (A) In vivo lung colonization assay of EKPC and HIF1A^{-/-}EKPC cells. Measurements of *in vivo* bioluminescence are shown from day 7 to 23 after tail vein injection. All images were set at the same pseudocolor scale to show relative bioluminescent changes over time. **(B&C)** Representative H&E staining and quantification of lung metastasis in mice injected with EKPC and HIF1A^{-/-}EKPC cells. **** $p < 0.0001$ by paired t test. All experiments were carried out in triplicate. All bar graphs represent mean and error bars are s.e.m.

Supplementary Figure 9 :



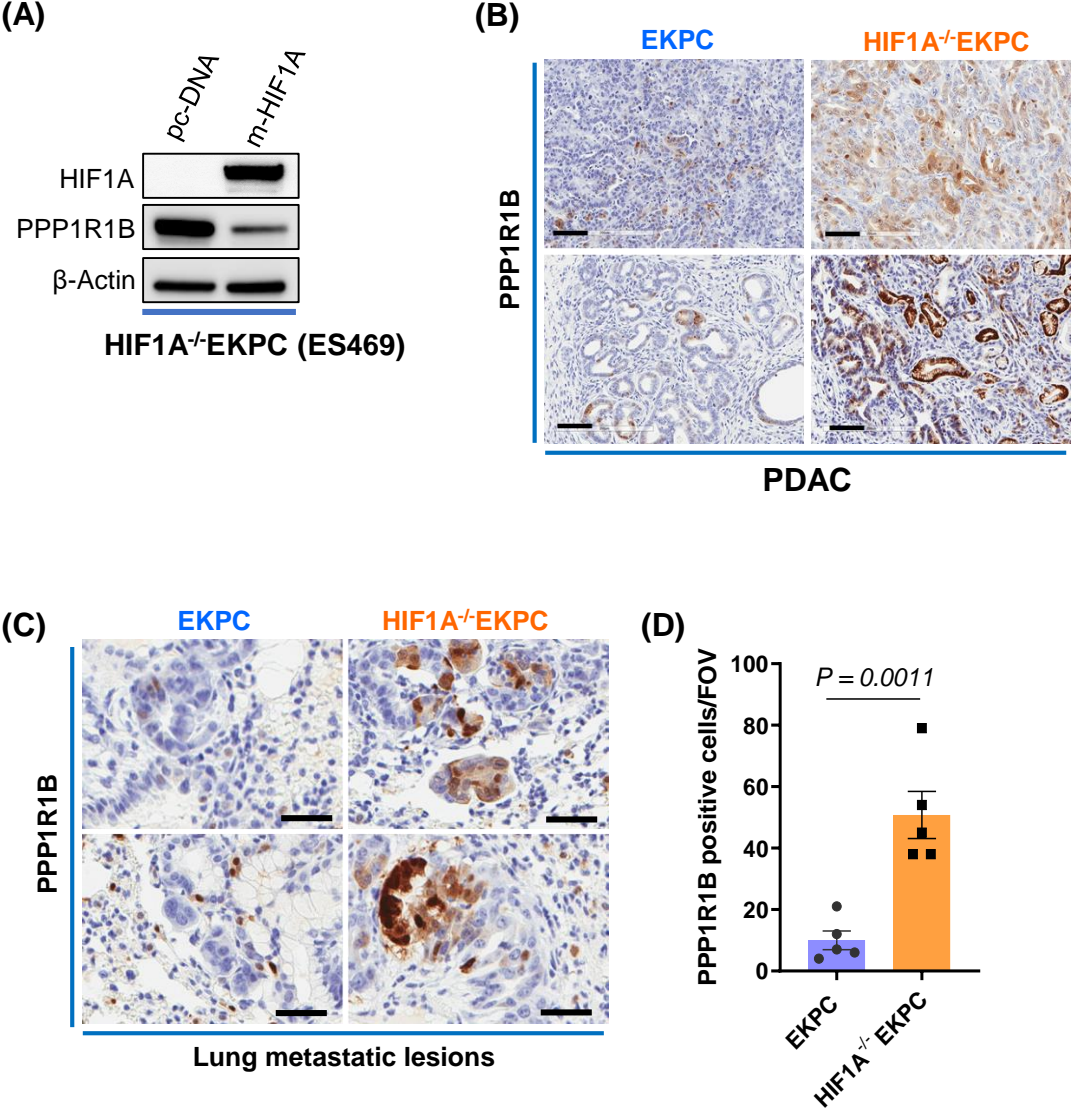
Supplementary Figure 9 : The Disease and Function IPA heatmap analysis of HIF1A^{-/-}EKPC vs EKPC cells. Differentially regulated proteins involved in cell movement, invasion, migration, cell contact and cell binding are ranked based on log₂fold change. 48 of 90 genes have measurement direction consistent with increase in cell movement. 44 of 79 genes have measurement direction consistent with increase in migration of cells. 25 of 41 genes have measurement direction consistent with increase in invasion of cells. 6 of 6 genes have measurement direction consistent with decrease in Cell-cell contact. 5 of 7 genes have measurement direction consistent with decrease in binding of cancer cell lines.

Supplementary Figure 10 :



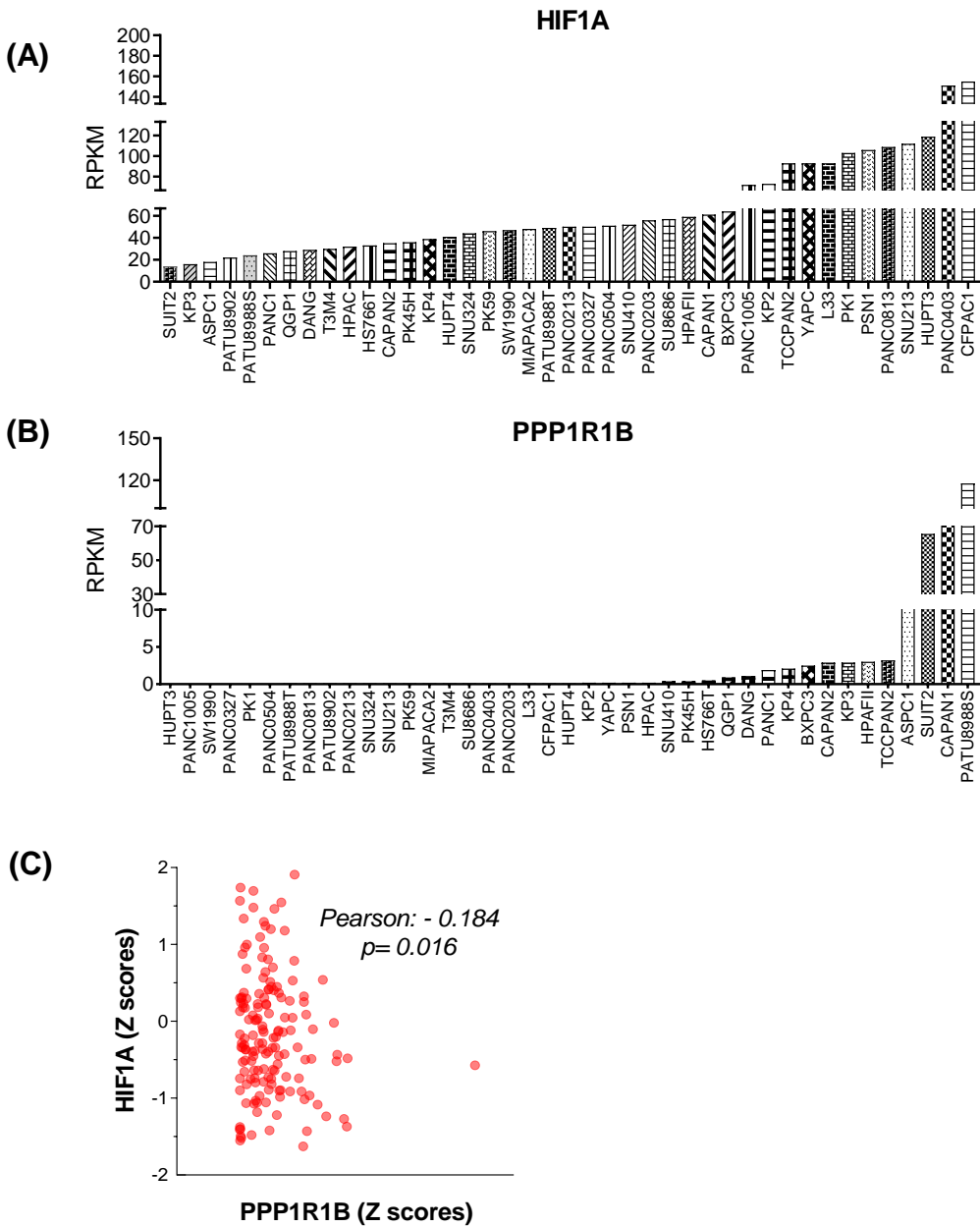
Supplementary Figure 10: (A&B): TCGA data set analysis of PPP1R1B expression in multiple tumor versus normal tissues. (COAD: Colon Adenocarcinoma, READ: Rectum Adenocarcinoma, LUAD: Lung adenocarcinoma, OV: Ovarian Serous Adenocarcinoma, PRAD: Prostate Adenocarcinoma, STAD: Stomach Adenocarcinoma, THCA: Thyroid Cancer, UCEC: Uterine Corpus Endometrial Carcinoma, UCS: Uterine Carcinosarcoma). The differential analysis is based on the selected datasets (TCGA tumors vs TCGA normal + GTEx normal); * p<0.05

Supplementary Figure 11 :



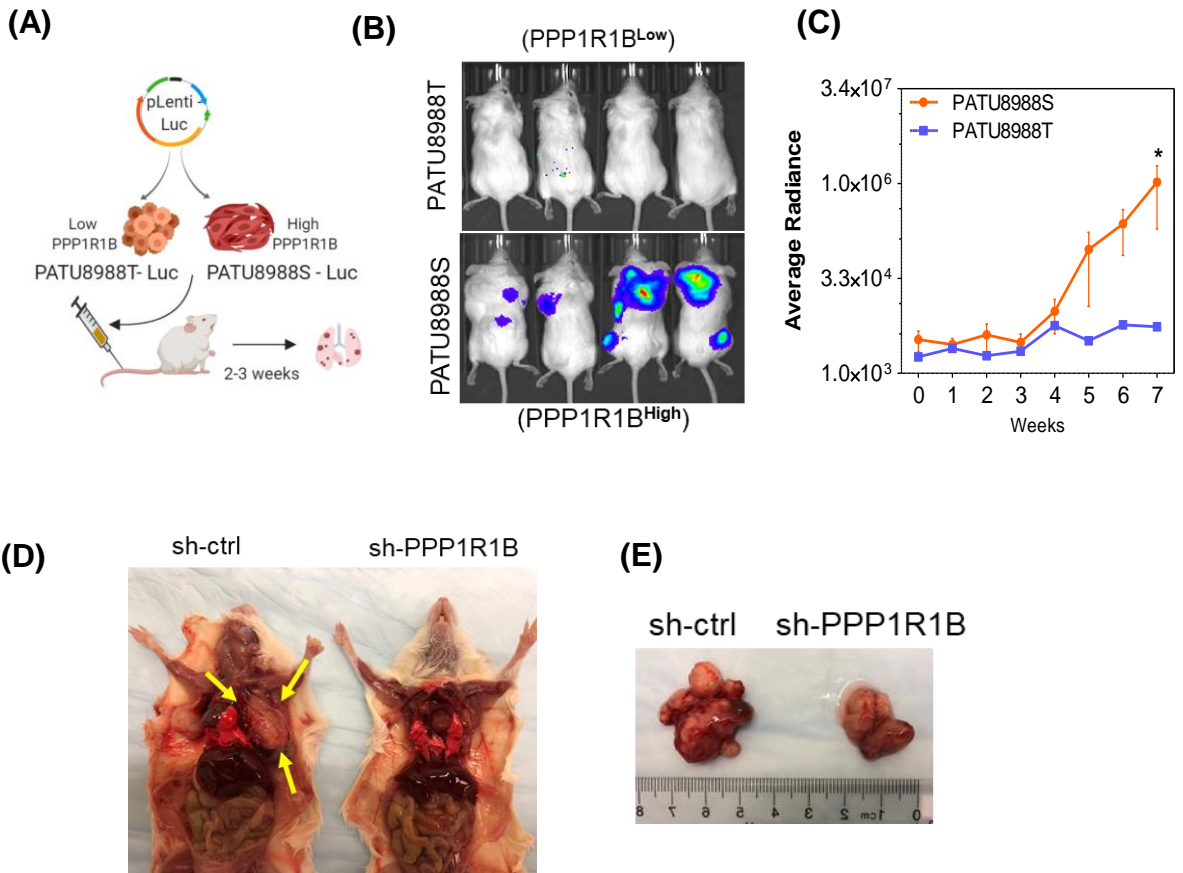
Supplementary Figure 11 : (A) Immunoblot analysis of PPP1R1B in ES469 (HIF1A^{-/-}EKPC) cells with and without ectopic HIF1A expression (B) Immunohistochemical staining of Ppp1r1b in pancreatic tumors from EKPC and HIF1A^{-/-}EKPC mouse (Scale bar:50 μm). (C) PPP1R1B positive tumor cells in sections from lung metastatic lesions from EKPC and HIF1A^{-/-}EKPC mice (n=5), representative images, Bar 50 μm. (D) Quantification of PPP1R1B+ cells in lung metastatic lesions sections (n = 5 field of vision for each section). P = 0.0011 by t test analysis.

Supplementary Figure 12 :



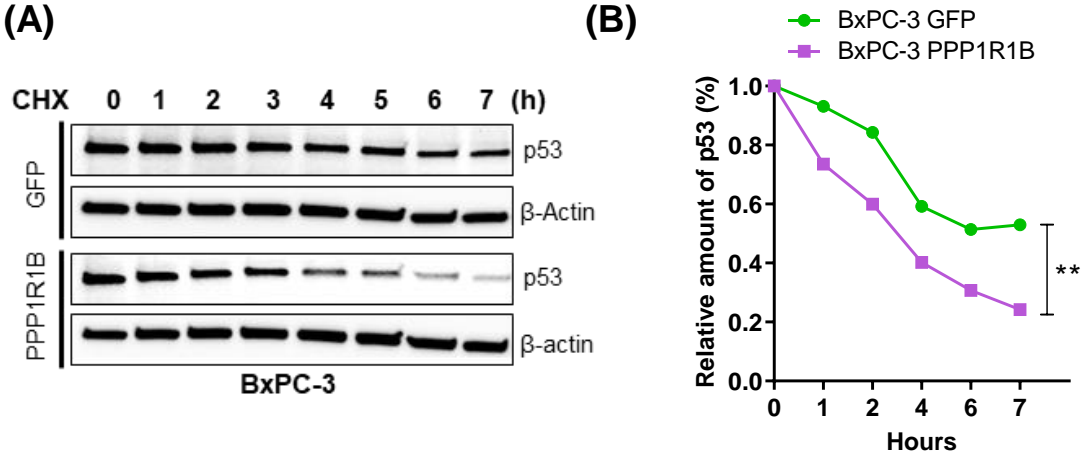
Supplementary Figure 12 : Comparative gene expression analysis of HIF1A **(A)** and PPP1R1B **(B)** levels in human pancreatic cancer cell lines derived from CCLE data base. **(C)** Co-expression analysis between HIF1A and PPP1R1B gene in 178 pancreatic cancer patients (TCGA) showing a negative correlation (Pearson coefficient -0.184; $p=0.016$ by paired t test). Each dot represents HIF1A and PPP1R1B gene pair.

Supplementary Figure 13:



Supplementary Figure 13: *In vivo* lung colonization assay of PATU8988T and PATU8988S cell lines. **(A & B)** Schematics of *in vivo* lung colonization assay for metastatic burden of PATU8988T (Ppp1r1b-low) and PATU8988S (Ppp1r1b-high) cells. (n=5 each experimental group). Representative image on day 93 post injection **(C)** Quantitative analysis of metastatic cells in whole body by bioluminescence analysis is shown as means \pm SEM; * $p < 0.05$ **(D)** Knock down of PPP1R1B by sh.PPP1R1B can reduce tumor metastasis (A) Tumor nodules formed by PATU8988S+sh.Ctrl and PATU8988S+sh.PPP1R1B cells upon tail vein injection (indicated by arrows). PPP1R1B depletion by sh.PPP1R1B led to significantly reduced tumor progression and metastasis burden **(E)** Comparative size of tumors isolated from NOD/SCID after injecting PATU8988S+sh.Ctrl and PATU8988S+sh.PPP1R1B cells.

Supplementary Figure 14:



Supplementary Figure 14: (A) Western blot analysis of Chase assay of p53 in PATU8988T cells expressing PPP1R1B or GFP. β -ACTIN was used as control. (B) Quantification of signal intensity from the Chase experiments.